

Theoretical analysis of force, pressure and energy distributions of bulk oil palm kernels along the screwline of a mechanical screw press FL 200

A. Kabutey^{1,*}, D. Herak¹, C. Mizera¹ and P. Hrabec²

¹Czech University of Life Sciences Prague, Department of Mechanical Engineering, Faculty of Mechanical Engineering, Kamycka 129, CZ165 00 Prague, Czech Republic

²Czech University of Life Sciences Prague, Department of Material Sciences and Manufacturing Technology, Kamycka 129, CZ165 21 Prague, Czech Republic

*Correspondence: kabutey@tf.czu.cz

Abstract. The present study is a follow-up of the previously published study on the mathematical description of loading curves and deformation energy of bulk oil palm kernels under compression loading, aimed at determining theoretically the amounts of force, pressure and energy along the screw lamella positions SL_p of the screw press FL 200 by applying the tangent curve mathematical model and the screwline geometry parameters (screw shaft diameter, screw inner and outer diameters, screw pitch diameter and the screw thickness). The fitting curve value F_v of the tangent mathematical model was further examined at $F_v = 2$ and $F_v = 3$ by identifying the force, deformation, stress and compression coefficients at varying vessel diameters D_v and initial pressing heights H_t of the bulk oil palm kernels. Based on the results of the stepwise regression analysis, the amounts of the theoretical deformation energy T_{DE} in linear pressing as well as the theoretical force F_r , pressure P_r and energy SL_E of the screw press FL 200 were statistically significant (P -value < 0.05) or (F -value $>$ significance F) in relation to the predictors (H_t , D_v , F_v and SL_p). The coefficient of determination (R^2) values between 61 and 86% were observed for the determined regression models indicating that the responses T_{DE} , F_r , P_r and SL_E can accurately be predicted by the corresponding predictors. The normal probability plots of the responses approximately showed a normal distribution.

Key words: experimental data, mathematical model, screw geometry parameters, compression loading, responses and predictors.

INTRODUCTION

Advanced oil extraction techniques such as microwave-assisted extraction, ultrasound-assisted extraction and pressurized liquid extraction are alternative oil extraction techniques to replace the conventional oil extraction methods namely solvent (hexane) extraction and mechanical pressing. These new extraction techniques provide several advantages over the traditional processes including shorter extraction time, reduced energy, greener solvents, less solvent use, full automation, greater reliability and environmentally friendly (Dutta et al., 2015; Castejon et al., 2018; Pandey & Shrivastava

2018). In spite of the advantages underlined, the application of these modern techniques in developing countries is very limited due to the high cost and operational skills.

The mechanical pressing (screw press or expeller) is more popular in developing countries due to the several advantages including simple equipment and sturdy in construction, easy maintenance, semi-skilled operator, easy adaption to processing other oilseeds, continuous oil process and chemical free protein of by-product (seedcake) (Kartika et al., 2010; Singh & Bargale 2000; Pradhan et al., 2011; Karaj & Muller 2011; Mridula et al., 2015; Liu et al., 2016; Uitterhaegen & Evon, 2017). Several efforts have been considered to improving the performance of mechanical screw press or expellers through modifications in press design and optimization of process variables as well as physical, thermal and chemical pretreatments. These efforts have helped to increase oil recovery levels from 50% to 80% for various oilseeds (Singh & Bargale 2000; Deli et al., 2011; Karaj & Muller 2011; Pradhan et al., 2011). In achieving higher oil extraction efficiency of the mechanical screw pressing, continuous research is still needed to understand the whole process. Theoretical analysis of the screw press configuration and design parameters (screw pitch diameter, pitch angle, screw thickness and screw shaft inner and outer diameters) in terms of pressure requirement is one of the research approaches (Herak et al., 2010; Sayin et al., 2015; Shankali et al., 2017; Pradhan et al., 2017; Bogaert et al., 2018). This, however, requires an in-depth knowledge of the linear compression process (Gupta & Das, 2007; Lysiak, 2007; Herak et al., 2013; Divisova et al., 2014; Demirel et al., 2017).

In the linear compression process, the deformation of the bulk oilseeds at varying initial pressing heights and vessel diameters in relation to the compression force and speed is examined. Based on the experimental dependency between the force and deformation curves of the bulk oilseeds/kernels, the tangent curve mathematical model can be used to describe the linear compression process (Herak et al., 2013; Sigalingging et al., 2014, 2015). The model can also be applied to the non-linear process (mechanical screw press FL 200) to theoretically analyze the pressure and energy requirements (Herak et al., 2010; Kabutey et al., 2016). The mechanical screw press FL 200 with 44 lamellas along the screwline can be divided into seven pressing positions, and for each pressing position, the mechanical behaviour (the dependency between the force and deformation curve) of the bulk oilseeds/kernels can be described where the theoretical force, pressure and energy can be determined. At the moment, the screw press FL 200 has not been used to process or recover the kernel oil which is semi-solid at room temperature compared to other vegetable oils that can easily be processed using the screw press FL 200. It is based on this background that the present study is essential to understand theoretically the mechanical behaviour of the bulk kernels along the screwline of screw press FL 200.

The present study, however, is a continuation of the previous study (Kabutey et al., 2018) aimed at analyzing the theoretical deformation energy of the bulk kernels based on the fitting curve values of the tangent mathematical model, determining the stress and compression coefficients of the tangent mathematical model and determining the theoretical amounts of force, pressure and energy along the screwline or screw lamella positions of screw press FL 200.

MATERIALS AND METHOD

Sample and compression test

Bulk oil palm kernels of moisture content of 9% w.b. were used for the compression test. The pressing vessels of diameters D_v 60, 80 and 100 mm with a plunger together with the universal compression-testing machine (ZDM 50, Czech Republic) were used to recover the kernel oil from the bulk kernels at initial pressing heights H_t 40, 60 and 80 under a maximum load of 200 kN and a speed of 5 mm min^{-1} (Fig. 1) (Kabutey et al., 2018).

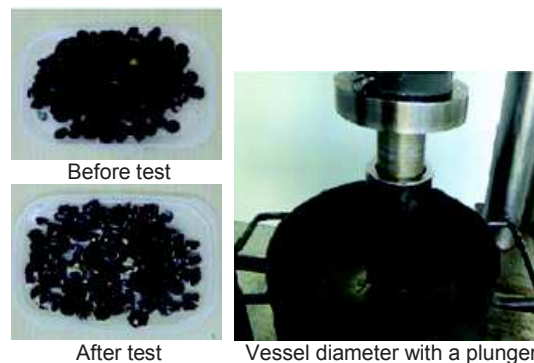


Figure 1. Compression test of bulk oil palm kernels for recovering the kernel oil.

Parameters obtained/calculated from the compression test

The deformation of the bulk kernels as well as the dependency between the force and deformation curves at varying D_v and H_t were obtained from the compression test. The percentage kernel oil and deformation energy T_{DE} were calculated as indicated in our previous publication (Kabutey et al., 2018).

Theoretical description of experimental curves

The theoretical description of the force and deformation curves of the bulk kernels was also described based on the tangent curve mathematical model (Herak et al., 2013; Sigalingging et al., 2014, 2015; Kabutey et al., 2018) by determining the force A (kN) and deformation B (mm^{-1}) coefficients at varying D_v and H_t of the bulk oil palm kernels (Kabutey et al., 2018). Here, the tangent curve model fitting value F_v was examined only at $F_v = 1$ (-). The present study, however, further evaluated $F_v = 2$ and $F_v = 3$ respectively to accurately compare the theoretical amounts of T_{DE} in linear pressing as well as the amounts of force F_r , pressure P_r and energy SL_E along the screwline of screw press FL 200.

Determination of the theoretical amounts of F_r , P_r and SL_E

The average stress and compression coefficients of the tangent curve mathematical model (Herak et al., 2013; Kabutey et al., 2016) were calculated. These coefficients and the expression of the cross-sectional area of the screwline were used to determine the theoretical amounts of F_r , P_r and SL_E distributions along the screwline of the screw press FL 200 with 44 lamellas divided into seven positions (0–7) (Fig. 2) (Kabutey et al., 2010; 2016).

The screwline parameters (screw shaft diameter, screw inner and outer diameters, screw pitch diameter and the screw thickness) designed for processing jatropha seeds were considered for the bulk oil palm kernels. Here, the amounts of the theoretical volume, initial pressing height, deformation and compression ratio of the bulk kernels along the screwline of the screw press FL 200 were similar to jatropha bulk seeds (Kabutey et al., 2016). However, at $F_v = 1$ for $D_v = 60, 80$ and 100 (mm); the compression

ratio in the tangent curve model (Herak et al., 2013; Sigalingging et al., 2014, 2015; Kabutey et al., 2018) was divided by the pressing factor coefficients of 1.637, 2.14 and 2.89 (-). At $F_v = 2$ the pressing factor coefficients were 1.59, 1.88 and 2.42 while at $F_v = 3$ the values of 1.508, 1.825 and 1.254 were considered. It is worth indicating that the pressing factor coefficients were guessed to correspond to the maximum force of 200 kN at a speed of 5 mm min^{-1} applied to the bulk oil palm kernels during the compression test.

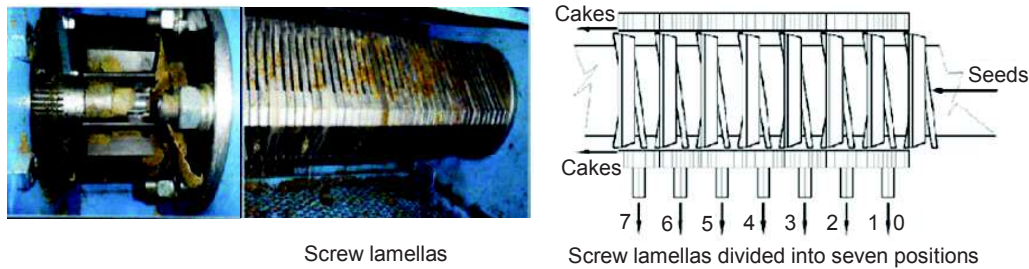


Figure 2. Screw press FL 200 geometry (Farmet, 2015; Kabutey et al., 2016).

Statistical analysis

The experimental and theoretical data obtained were analysed using the MathCad 14, IBM SPSS Statistics 25 and Statistica 13 by employing the general linear model and stepwise regression techniques.

RESULTS AND DISCUSSION

In the previously published study (Kabutey et al., 2018), the tangent curve model fitting value $F_v = 1$ (-) was examined where the theoretical dependency between the force and deformation curves as well as deformation energy of the bulk oil palm kernels at varying vessel diameters $D_v = 60, 80$ and 100 mm and initial pressing heights $H_t = 40, 60$ and 80 mm were described. The present study, however, further examined $F_v = 2$ and $F_v = 3$ as indicated in Tables 1 to 3 respectively. The theoretical force A and deformation B coefficients at F_v values were statistically significant ($P \text{ values} > 0.05$) or values of $F\text{-critical} > F\text{-ratio}$ according to the Mathcad 14 program. From the results obtained, it was observed that the $D_v = 100 \text{ mm}$ at $H_t = 80 \text{ mm}$, the trigonometric function (\sin) instead of a (\tan) function of the tangent curve model (Herak et al., 2013; Sigalingging et al., 2014, 2015) best described the experimental data. In view of the above, the results $H_t = 80 \text{ mm}$ were not included in any further calculations due to the change of the trigonometric function. The average coefficients of force A (kN), deformation B (mm^{-1}), stress C (N mm^{-1}) and compression G (-) at varying H_t for each D_v are shown in Table 4. These coefficients showed both decreasing and increasing trends in relation to F_v values for all D_v . The results were statistically significant based on the linear regression analysis with a coefficient of determination values (R^2) between 40 to 77%. The average coefficients of C (N mm^{-1}) and G (-) were determined based on the expressions given by Herak et al., 2013; Sigalingging et al., 2014, 2015.

Table 1. Theoretical description of the experimental force-deformation curve for $D_v = 60$ mm

H_t (mm)	A (kN)	B (mm ⁻¹)	F_v (-)	F-ratio (-)	F-critical (-)	P -value (-)	R^2 (-)
40	19.88	0.058	1	0.024	3.853	0.876	0.997
40	16.68	0.058	1	0.015	3.863	0.903	0.999
60	13.87	0.039	1	$2.067 \cdot 10^{-3}$	3.848	0.989	0.999
60	16.19	0.039	1	$6.149 \cdot 10^{-3}$	3.848	0.938	1
80	14.27	0.03	1	$8.813 \cdot 10^{-5}$	3.862	0.993	0.999
80	13.3	0.03	1	$1.363 \cdot 10^{-5}$	3.862	0.997	0.999
40	11.98	0.052	2	0.01	3.853	0.919	0.999
40	9.519	0.052	2	0.069	3.863	0.792	0.997
60	6.496	0.036	2	0.18	3.848	0.671	0.993
60	9.393	0.036	2	0.131	3.848	0.717	0.996
80	9.318	0.027	2	0.242	3.862	0.623	0.989
80	6.856	0.028	2	0.236	3.862	0.627	0.991
40	12.47	0.047	3	0.039	3.853	0.844	0.998
40	9.158	0.047	3	0.156	3.863	0.693	0.994
60	5.027	0.033	3	0.295	3.848	0.587	0.988
60	9.313	0.032	3	0.229	3.848	0.632	0.993
80	10.81	0.024	3	0.425	3.862	0.515	0.982
80	5.821	0.025	3	0.424	3.862	0.515	0.986

F-ratio < F-critical or P -value > 0.05 is significant (Mathsoft 2014); D_v is the vessel diameter (mm); H_t is the initial pressing height of the bulk palm kernels (mm); A is the force coefficient of mechanical behaviour (kN); B is the deformation coefficient of mechanical behaviour (mm⁻¹); F_v is the fitting curve value (-); F-ratio is the value of the F test, F-critical is the value that compares a pair of models, R^2 is the coefficient of determination (-).

Table 2. Theoretical description of the experimental force-deformation curve for $D_v = 80$ mm

H_t (mm)	A (kN)	B (mm ⁻¹)	F_v (-)	F-ratio (-)	F-critical (-)	P -value (-)	R^2 (-)
40	24.84	0.061	1	$2.21 \cdot 10^{-3}$	3.848	0.963	1
40	27.51	0.064	1	$2.251 \cdot 10^{-3}$	3.848	0.962	0.999
60	25.7	0.041	1	$2.618 \cdot 10^{-3}$	3.847	0.959	1
60	23.56	0.041	1	$1.513 \cdot 10^{-3}$	3.848	0.969	0.999
80	23.69	0.032	1	$1.879 \cdot 10^{-4}$	3.847	0.989	0.999
80	23.39	0.032	1	$1.031 \cdot 10^{-4}$	3.847	0.992	0.999
40	19.45	0.053	2	0.154	3.848	0.694	0.996
40	25.82	0.054	2	0.207	3.848	0.649	0.995
60	21.9	0.036	2	0.146	3.847	0.703	0.996
60	19.97	0.035	2	0.231	3.848	0.631	0.992
80	22.38	0.027	2	0.192	3.847	0.661	0.993
80	19.94	0.028	2	0.171	3.847	0.68	0.993
40	27.92	0.046	3	0.23	3.848	0.631	0.993
40	48.62	0.045	3	0.297	3.848	0.586	0.992
60	35.16	0.03	3	0.244	3.847	0.622	0.992
60	32.74	0.03	3	0.345	3.848	0.557	0.987
80	43.48	0.022	3	0.31	3.847	0.578	0.988
80	32.55	0.023	3	0.285	3.847	0.593	0.988

Table 3. Theoretical description of the experimental force-deformation curve for $D_v = 100$ mm

H_t (mm)	A (kN)	B (mm ⁻¹)	F_v (-)	F-ratio (-)	F-critical (-)	P -value (-)	R^2 (-)
40	39.67	0.059	1	0.053	3.848	0.818	0.999
40	39.3	0.057	1	$3.539 \cdot 10^{-3}$	3.848	0.953	1
60	40.04	0.04	1	0.016	3.848	0.9	0.999
60	38.11	0.041	1	0.024	3.848	0.876	0.999
80	44.47	0.032	1	$2.866 \cdot 10^{-3}$	3.848	0.957	0.999
80	43.81	0.033	1	0.034	3.848	0.855	0.999
40	65.49	0.044	2	0.1	3.848	0.752	0.997
40	53.63	0.045	2	0.207	3.848	0.65	0.997
60	74.85	0.03	2	0.145	3.848	0.704	0.995
60	63.7	0.031	2	0.124	3.848	0.725	0.995
80	106.5	0.022	2	0.186	3.848	0.666	0.995
80	116.2	0.022	2	0.108	3.848	0.743	0.996
40	413.8	0.028	3	0.165	3.848	0.684	0.994
40	197.6	0.033	3	0.297	3.848	0.586	0.995
60	846.1	0.016	3	0.236	3.848	0.628	0.99
60	442.5	0.019	3	0.211	3.848	0.646	0.991
*80	13,940	$5.488 \cdot 10^{-3}$	3	0.299	3.848	0.584	0.99
*80	14,060	$5.668 \cdot 10^{-3}$	3	$3.247 \cdot 10^{-3}$	3.848	0.955	0.992

* Trigonometric function (*sin*) instead of a (*tan*) function of the tangent models best described the experimental data.

Table 4. Cumulative amounts of the tangent curve model coefficients at $H_t = 40, 60$ and 80 mm

D_v (mm)	F_v (-)	A (kN)	B (mm ⁻¹)	C (N mm ⁻²)	G (-)
60	1	15.70 ± 1.53	0.04 ± 0.00	4.36 ± 0.43	2.35 ± 0.00
80		24.78 ± 1.20	0.05 ± 0.00	3.87 ± 0.19	2.51 ± 0.03
100		40.90 ± 0.70	0.04 ± 0.00	4.09 ± 0.07	2.45 ± 0.05
60	2	30.98 ± 4.88	0.05 ± 0.00	4.16 ± 0.68	2.00 ± 0.02
80		32.72 ± 3.77	0.03 ± 0.00	4.14 ± 0.53	2.04 ± 0.03
100		46.87 ± 3.44	0.03 ± 0.00	5.56 ± 0.48	2.05 ± 0.04
60	3	8.77 ± 2.97	0.03 ± 0.00	2.44 ± 0.82	1.93 ± 0.03
80		36.75 ± 8.03	0.03 ± 0.00	5.74 ± 1.25	1.81 ± 0.03
100		475.00 ± 219.13	0.02 ± 0.00	47.50 ± 21.91	1.14 ± 0.13

Table 5. Cumulative amounts of T_{DE} at $H_t = 40, 60$ and 80 mm

D_v (mm)	F_v (-)	T_{DE} (J)
60		990.74 ± 41.77
80	1	818.39 ± 53.29
100		709.40 ± 108.73
60		1,245.48 ± 34.48
80	2	1,041.10 ± 39.85
100		947.05 ± 42.69
60		1,579.50 ± 20.03
80	3	1,445.43 ± 47.09
100		1,148.56 ± 41.44

The cumulative values of the theoretical deformation energy T_{DE} (J) of bulk oil palm kernels based on the tangent curve model (Herak et al., 2013; Kabutey et al., 2018; Sigalingging et al., 2014, 2015) and the regression analysis are given in Tables 5 to 8.

Table 6. Regression statistics of the dependent variable: T_{DE}

Model parameters	R	R Square	Adjusted R Square	Standard error of the estimate
H_t, F_v, D_v	0.960 ^a	0.922	0.917	114.57

^a Predictors: (Constant): Height H_t , vessel diameter D_v , tangent curve model fitting value F_v .

Table 7. Anova analysis of the dependent variable: T_{DE}

Model parameters	Sum of squares	Degree of freedom	Mean square	F	Significance F
Regression	7,399,540.422	3	2,466,513.474	187.914	0.000 ^a
Residual	630,036.842	48	13,125.768		
Total	8,029,577.264	51			

Table 8. Regression coefficients of the dependent variable: T_{DE}

Model parameters	Unstandardized coefficients		Standardized coefficients <i>Beta</i>	t-value	P-value
	<i>B</i>	<i>Standard error</i>			
Constant	-785.227	112.174		-7.000	0.000
H_t	16.432	0.987	0.675	16.640	0.000
D_v	15.064	0.987	0.619	15.255	0.000
F_v	-142.997	19.749	-0.294	-7.241	0.000

The linear regression model expressing the response T_{DE} of bulk oil palm kernels in linear pressing at a maximum force of 200 kN and a speed of 5 mm min⁻¹ is described in Eq. 1 as follows:

$$T_{DE}(J) = -785.227 + 16.432 \cdot H_t + 15.064 \cdot D_v - 142.997 \cdot F_v \quad (1)$$

Eq. 1 is significant based on the fact that the significance F value of the Anova results was less than the 5% significance level or the F value was much greater than the significance F. The coefficient of determination was 0.922, that is, 92.2% of the variation in the theoretical deformation energy is explained by the predictors (H_t , D_v and F_v). The normal probability plot of the response T_{DE} is shown in Fig. 3. The data points followed the normal distribution assumption with no strong deviations.

The theoretical amounts of the force F_r , pressure P_r and energy SL_E of bulk oil palm kernels along the screw lamella positions SL_p of screw press FL 200 are indicated in Tables 9 to 11 and graphically described in Figs 4 to 6. These amounts were determined based on the tangent curve model (Herak et al., 2013; Kabutey et al., 2018; Sigalingging et al., 2014, 2015), screwline geometry information (screw shaft diameter, screw inner and outer diameters, screw pitch diameter and the screw thickness) and other mathematical equations as described in our previous publication on jatropha bulk oilseeds (Kabutey et al., 2016). The cumulative amounts of F_r , P_r and SL_E are also given in Tables 12 to 14 respectively.

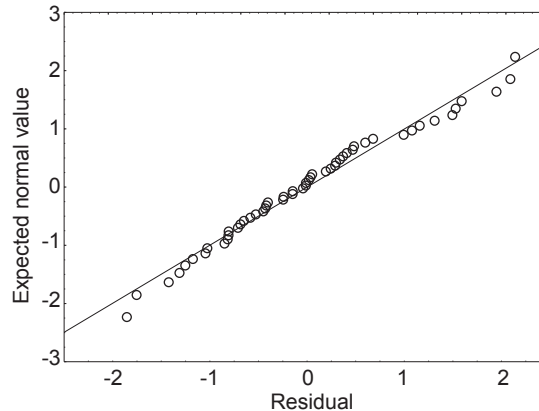
**Figure 3.** Normal probability plot of the regression standardized residual of the dependent variable: T_{DE} (J).

Table 9. Calculated parameters at the screw lamellas positions for $F_v = 1$

SL_p (-)	D_v (mm)	F_r (kN)	P_r (MPa)	SL_E (J)
0	60	0	0	0
1	60	10.32	2.129	102.963
2	60	24.01	7.681	179.566
3	60	25.43	8.575	180.461
4	60	28.47	10.878	180.025
5	60	30.23	12.388	178.631
6	60	35.55	17.852	170.587
7	60	46.58	34.581	145.322
0	80	0	0	0
1	80	12.75	2.629	99.442
2	80	26.11	8.321	163.667
3	80	27.17	9.161	163.534
4	80	29.46	11.257	161.022
5	80	30.71	12.585	158.59
6	80	34.18	17.162	148.187
7	80	40.13	29.794	121.116
0	100	0	0	0
1	100	14.63	3.018	86.216
2	100	27.19	8.666	135.621
3	100	28.04	9.456	134.973
4	100	29.82	11.396	131.756
5	100	30.76	12.605	129.153
6	100	33.22	16.679	119.109
7	100	37.02	27.468	95.216

F_v : fitting curve value; SL_p : screw lamellas positions; D_v : vessel diameter; P_r : force; F_r : pressure; SL_E : energy at screw lamellas positions.

Table 11. Calculated parameters at the screw lamellas positions for $F_v = 3$

SL_p (-)	D_v (mm)	F_r (kN)	P_r (MPa)	SL_E (J)
0	60	0	0	0
1	60	1.634	0.337	8.548
2	60	16.11	5.134	58.853
3	60	18.4	6.204	63.732
4	60	24.2	9.247	73.99
5	60	27.9	11.435	79.351
6	60	40.5	20.334	92.5
7	60	72.14	53.561	106.147
0	80	0	0	0
1	80	2.822	0.582	12.701
2	80	20.2	6.439	71.036
3	80	22.38	7.546	75.414
4	80	27.48	10.501	83.773
5	80	30.49	12.494	87.647

Table 10. Calculated parameters at the screw lamellas positions for $F_v = 2$

SL_p (-)	D_v (mm)	F_r (kN)	P_r (MPa)	SL_E (J)
0	60	0	0	0
1	60	4.682	0.966	31.655
2	60	21.09	6.721	105.076
3	60	23	7.755	109.149
4	60	27.48	10.499	116.335
5	60	30.13	12.348	119.351
6	60	38.32	19.24	123.924
7	60	55.46	41.178	118.872
0	80	0	0	0
1	80	5.866	1.21	34.231
2	80	23.09	7.358	105.201
3	80	24.85	8.378	108.479
4	80	28.82	11.015	113.747
5	80	31.09	12.741	115.632
6	80	37.69	18.927	116.962
7	80	50.02	37.137	107.03
0	100	0	0	0
1	100	7.106	1.465	32.928
2	100	24.53	7.817	93.79
3	100	26.09	8.797	96.07
4	100	29.5	11.274	99.287
5	100	31.38	12.86	100.136
6	100	36.59	18.375	99.094
7	100	45.46	33.747	87.395

Table 12. Cumulative amounts of F_r (kN) at SL_p

D_v (mm)	$F_v = 1$ (-)	$F_v = 2$ (-)	$F_v = 3$ (-)
60	200.59	200.16	200.88
80	200.51	201.43	200.80
100	200.68	200.66	200.28

F_r : force; SL_p : screw lamella positions (-); D_v : vessel diameter (mm); F_v : fitting curve value (-).

Table 13. Cumulative amounts of P_r (MPa) at SL_p

D_v (mm)	$F_v = 1$ (-)	$F_v = 2$ (-)	$F_v = 3$ (-)
60	94.084	98.707	106.252
80	90.909	96.766	100.371
100	89.288	94.335	96.33

P_r : pressure.

Table 11 (continued)

6	80	39.62	19.893	95.197
7	80	57.81	42.916	96.175
0	100	0	0	0
1	100	4.269	0.88	16.224
2	100	23.11	7.366	75.5
3	100	25.01	8.432	78.933
4	100	29.2	11.157	84.841
5	100	31.52	12.917	87.198
6	100	38.03	19.095	90.238
7	100	49.14	36.483	84.25

Table 14 Cumulative amounts of SL_E (J) at SL_p

D_v (mm)	$F_v = 1$ (-)	$F_v = 2$ (-)	$F_v = 3$ (-)
60	1,137.555	724.362	483.121
80	1,015.558	701.282	521.943
100	832.044	608.7	517.184

SL_E : energy at screw lamellas positions.

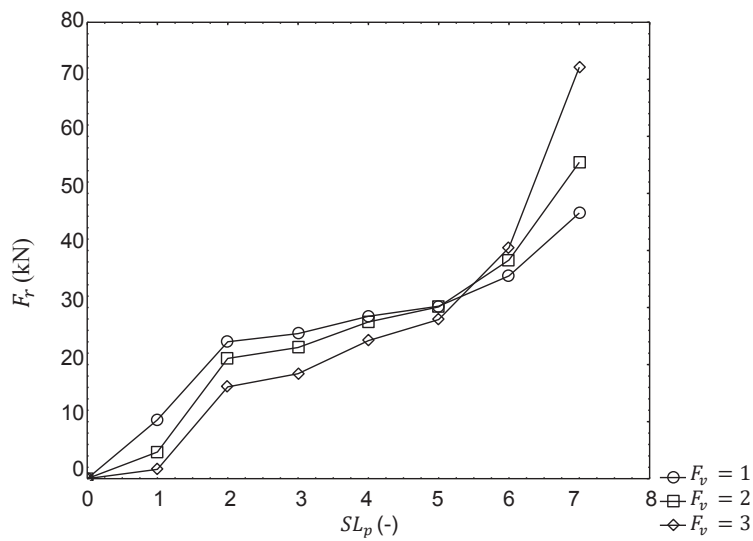


Figure 4. Relationship between F_r and SL_p in relation to F_v for $D_v = 60$ mm.

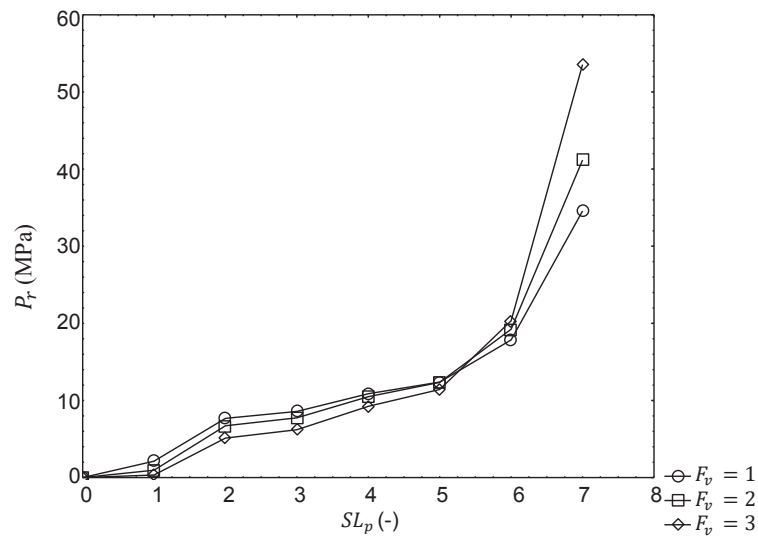


Figure 5. Relationship between P_r and SL_p in relation to F_v for $D_v = 60$ mm.

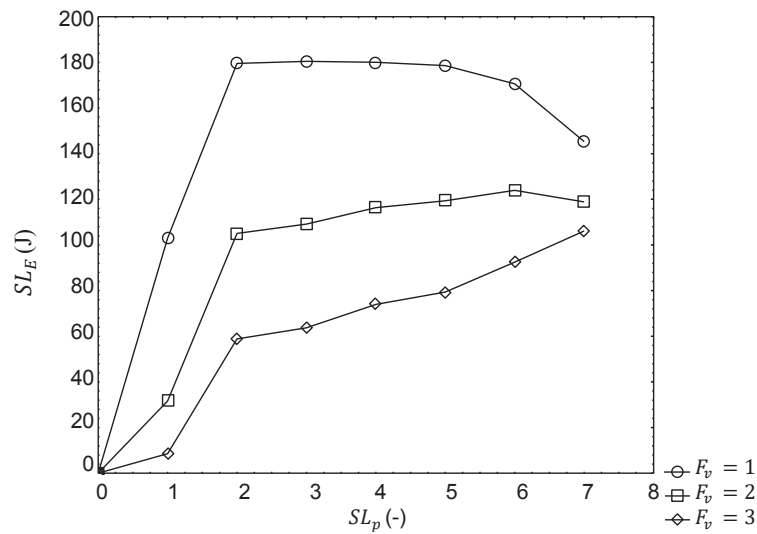


Figure 6. Relationship between SL_E and SL_p in relation to F_v for $D_v = 60$ mm.

The results of the regression analysis employing the stepwise method for the responses or dependent variables (F_r , P_r and SL_E) and the predictors or independent variables (SL_p , D_v and F_v) are given in Tables 15 to 23 respectively. The response F_r turned out to be predicted only by the SL_p as shown in Tables 15 to 17.

Table 15. Regression statistics of the dependent variable: F_r (kN)

Model parameter	R	R Square	Adjusted R Square	Standard error of the estimate
SL_p	0.931 ^a	0.867	0.865	5.735

^a Predictor: (Constant); SL_p : screw lamella positions (-).

Table 16. Anova analysis of the dependent variable: F_r (kN)

Model parameters	Sum of squares	Degree of freedom	Mean square	F	Significance F
Regression	15,015.391	1	15,015.391	456.582	0.000 ^a
Residual	2,302.057	70	32.887		
Total	17,317.448	71			

Table 17. Regression coefficients of the dependent variable: F_r (kN)

Model parameters	Unstandardized coefficients		Standardized coefficients	t-value	P-value
	B	Standard error			
Constant	3.024	1.234		2.451	0.017
SL_p	6.303	0.295	0.931	21.368	0.000

The regression equation of the response F_r is given in Eq. 2 as follows:

$$F_r(kN) = 3.024 + 6.303 \cdot SL_p \quad (2)$$

Eq. 2 is significant based on the fact that the significance F value of the Anova results was less than the 5% significance level or the F value was much greater than the significance F. The coefficient of determination was 0.867, that is, 86.7% of the variation in the response F_r is explained by the predictor SL_p . The response P_r also correlated with the SL_p as shown in Tables 18 to 20.

Table 18. Regression statistics of the dependent variable: P_r (MPa)

Model parameter	R	R Square	Adjusted R Square	Standard error of the estimate
SL_p	0.875 ^b	0.765	0.762	5.609

^b Predictor: (Constant), SL_p : screw lamella positions (-).

Table 19. Anova analysis of the dependent variable: P_r (MPa)

Model parameters	Sum of squares	Degree of freedom	Mean square	F	Significance F
Regression	7,173.121	1	7,173.121	228.028	0.000 ^a
Residual	2,202.003	70	31.457		
Total	9,375.124	71			

Table 20. Regression coefficients of the dependent variable: P_r (MPa)

Model parameters	Unstandardized coefficients		Standardized coefficients	t-value	P-value
	B	Standard error	Beta		
Constant	-3.204	1.207		-2.655	0.010
SL_p	4.356	0.288	0.875	15.101	0.000

The regression equation of the response P_r is given in Eq. 3 as follows:

$$P_r(MPa) = -3.204 + 4.356 \cdot SL_p \quad (3)$$

Eq. 3 is significant based on the fact that the significance F value of the Anova results was less than the 5% significance level or the F value was much greater than the significance F. The coefficient of determination was 0.875, that is, 87.5% of the variation in the response P_r was explained by the predictor SL_p . The response SL_E also correlated with predictors SL_p and F_v as shown in Tables 21 to 23.

Table 21. Regression statistics of the dependent variable: SL_E (J)

Model parameters	R	R Square	Adjusted R Square	Standard error of the estimate
SL_p, F_v	0.776 ^c	0.602	0.591	32.786

^c Predictors: (Constant), screw lamella positions, SL_p ; fitting curve value, F_v .

Table 22. Anova analysis of the dependent variable: SL_E (J)

Model parameters	Sum of squares	Degree of freedom	Mean square	F	Significance F
Regression	112,336.987	2	56,168.494	52.253	0.000 ^a
Residual	74,169.713	69	1,074.923		
Total	186,506.701	71			

Table 23. Regression coefficients of the dependent variable: SL_E (J)

Model parameters	Unstandardized coefficients		Standardized coefficients <i>Beta</i>	t-value	P-value
	<i>B</i>	<i>Standard error</i>			
Constant	104.954	11.804		8.891	0.000 ^c
SL_p	13.388	1.686	0.603	7.939	0.000 ^c
F_v	-30.477	4.732	-0.489	-6.440	0.000 ^c

The regression equation of the response SL_E is given in Eq. 4 as follows:

$$SL_E(J) = 104.954 + 13.388 \cdot SL_p - 30.477 \cdot F_v \quad (4)$$

Eq. 4 is significant based on the fact that significance F value of the Anova results was less than the 5% significance level or the F value was much greater than the significance F. The coefficient of determination was 0.602, that is, 60.2% of the variation in the response SL_E was explained by the predictors SL_p and F_v . The normal probability plots of the responses F_r , P_r and SL_E are shown in Figs 7 to 9. Approximately, the data points showed a normal distribution.

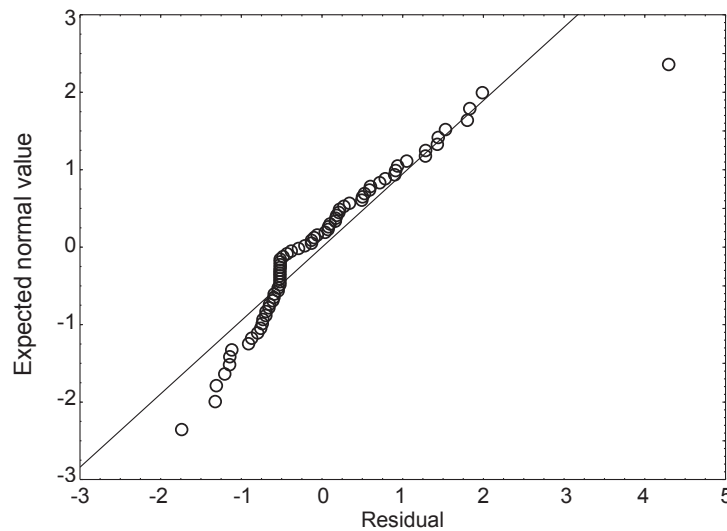


Figure 7. Normal probability plot of the regression standardized residual of the dependent variable: F_r (kN).

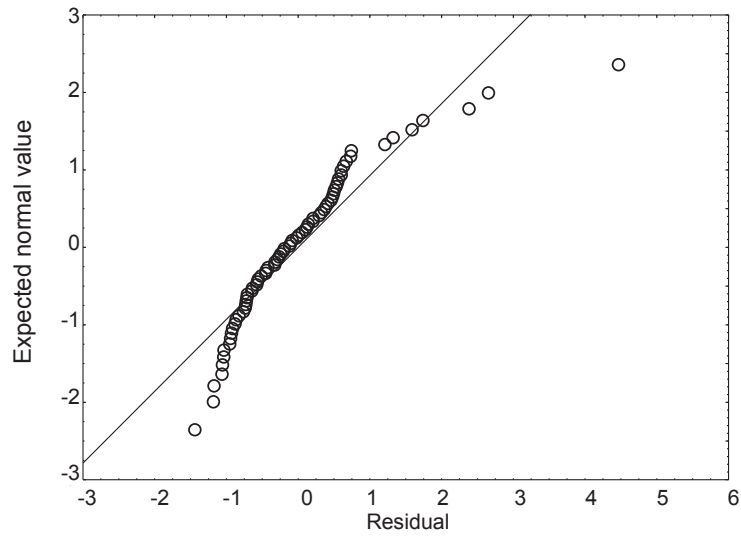


Figure 8. Normal probability plot of the regression standardized residual of the dependent variable: P_r (MPa).

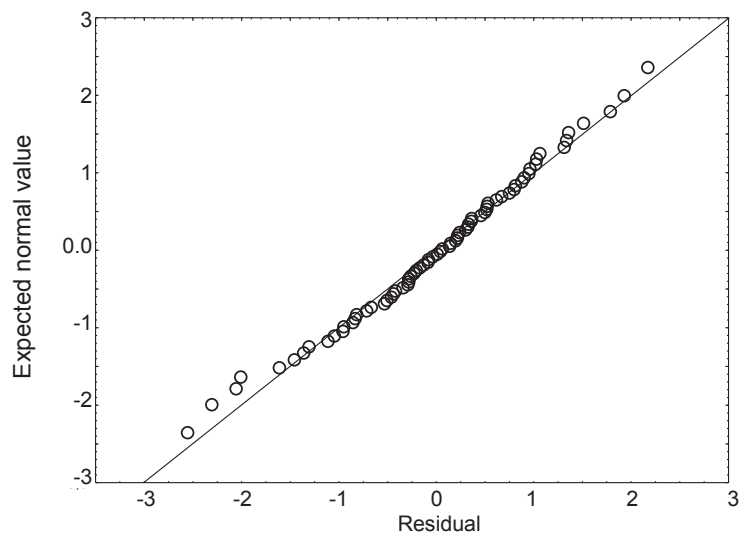


Figure 9. Normal probability plot of the regression standardized residual of the dependent variable: SL_E (J).

CONCLUSIONS

The average force, deformation, stress and compression coefficients were determined for describing bulk oil palm kernels at varying initial pressing heights, vessel diameters and fitting values of the tangent curve mathematical model. A linear regression model was described for the theoretical deformation energy of bulk oil palm kernels under compression loading based on the initial pressing heights of bulk kernels, vessel diameters and fitting values of the tangent curve models. Linear regression models were

also described for the theoretical force, pressure and energy of the bulk kernels along the screwline of the mechanical screw press FL 200 based on the screw lamella positions and fitting values of the tangent curve models. From the industrial/design point of view, the screw press FL 200 can be used to process a wide range of oilseeds such as jatropha seeds, rapeseeds, sunflower seeds and others by both cold-pressing and extrusion pressing. There is limited information in the literature about the cold-pressing and extrusion pressing of bulk oil palm kernels. Therefore, the present study results provide the background information for using the screw press FL 200 and Farnet Duo for processing bulk oil palm kernels as well as optimizing the process in terms of maximum kernel oil recovery and minimum energy input.

ACKNOWLEDGEMENTS. The research was financially supported by the project 'supporting the development of international mobility of research staff at CULS Prague' registration number: CZ.02.2.69/0.0/0.0/16_027/0008366.

REFERENCES

- Bargale, P.C., Wulfsohn, D., Irudayaraj, J., Ford, R.J. & Sosulski, F.W. 2000. Prediction of Oil Expression by Uniaxial Compression using Time-varying Oilseeds Properties. *Journal of Agricultural Engineering Research* **77**(2), 171–181.
- Bogaert, L., Mathieu, H., Mhemdi, H. & Vorobiev, E. 2018. Characterization of oilseeds mechanical expression in an instrumented pilot screw press. *Industrial Crops and Products* **121**, 106–113.
- Castejon, N., Luna, P. & Senorans, F.J. 2018. Alternative oil extraction methods from *Echium plantagineum* L, seeds using advanced techniques and green solvents. *Food Chemistry* **244**, 75–82.
- Deli, S., Farah Masturah, M., Tajul Aris, Y. & Wan Nadiah, W.A. 2011. The effects of physical parameters of the screw press oil expeller on oil yield from *Nigella sativa* L. seeds. *Journal International Food Research* **18**(4), 1367–1373.
- Demirel, C., Kabutey, A., Herak, D. & Gurdil, G.A.K. 2017. Numerical estimation of deformation energy of selected bulk oilseeds in compression loading, IOP Conference, Series: *Material Science Engineering* **237**(1), 1–5.
- Divisova, M., Herak, D., Kabutey, A., Sleger, V., Sigalingging, R. & Svatonova, T. 2014. Deformation curve characteristics of rapeseeds and sunflower seeds under compression loading. *Scientia Agriculturae Bohemica* **45**, 180–186.
- Dutta, R., Sarkar, U. & Mukherjee, A. 2015. Process optimization for the extraction of oil from *Crotalaria juncea* using three phase partitioning. *Industrial Crops and Products* **71**, 89–96.
- Farnet, 2015. Oil and Feed Tech, Jirinkova 276, Czech Republic
- Gupta, R.K. & Das, S.K., 2000. Fracture resistance of sunflower seed and kernel to compressive loading. *Food Engineering* **46**, 1–8.
- Herák, D., Kabutey, A., Divišová, M. & Simanjuntak, S. 2013. Mathematical model of mechanical behaviour of *Jatropha curcas* L, seeds under compression loading. *Biosystems Engineering* **114**(3), 279–288.
- Herak, D., Sedlacek, A. & Kabutey, A. 2010. Determination of the complete geometry of the worm extruder screwline for compressive pressing of the oil bearing crops. *Conference Proceeding, 4th International Conference TAE*, pp. 207–210.
- IBM Corp., Released 2017. IBM SPSS Statistics for Windows, Version 25.0. Armonk, NY: IBM Corp.

- Kabutey, A., Herak, D., Hanus, J., Choteborsky, R., Dajbych, O., Sigalingging, R. & Akangbe, O.L. 2016. Prediction of pressure and energy requirement of *Jatropha curcas* L. bulk seeds under non-linear pressing. *Conference Proceeding, 4th International Conference TAE*, pp. 262–269.
- Kabutey, A., Herak, D., Mizera, C. & Hrabě, P. 2018. Mathematical description of loading curves and deformation energy of bulk oil palm kernels. *Agronomy Research* **16**(4), 1686–1697.
- Karaj, S. & Muller, J. 2011. Optimizing mechanical oil extraction of *Jatropha curcas* L. seeds with respect to press capacity, oil recovery and energy efficiency. *Industrial Crops Products* **34**, 1010–16.
- Kartika, I.A., Pontalier, P.Y. & Rigal, L. 2010. Twin-screw extruder for oil processing of sunflower seeds: Thermo-mechanical pressing and solvent extraction in a single step. *Industrial Crops Products* **32**, 297–304.
- Liu, J., Gasmalla, M.A.A., Li, P. & Yang, R. 2016. Enzyme-assisted extraction processing from oilseeds: Principle, processing and application. *Innovative Food Science & Emerging Technologies* **35**, 184–193.
- Lysiak, G. 2007. Fracture toughness of pea: Weibull analysis. *International Journal of Food Engineering* **83**, 436–443.
- Mathsoft. 2014. Parametric Technology Corporation, Needham, MA02494, USA.
- Mridula, D., Barnwal, P. & Singh, K.K. 2015. Screw pressing performance of whole and dehulled flaxseed and some physico-chemical characteristics of flaxseed oil. *Journal of Food Science Technology* **52**, 1498–1506.
- Pandey, R. & Shrivastava, S.L. 2018. Comparative evaluation of rice bran oil obtained with two-step microwave assisted extraction and conventional solvent extraction. *Journal of Food Engineering* **218**, 106–114.
- Pradhan, R.C., Mishra, S., Naik, S.N., Bhatnagar, N. & Vijay, V.K. 2011. Oil expression from *Jatropha* seeds using a screw press expeller. *Biosystems Engineering* **109**, 158–166.
- Sayin, R., Martinez-Marcos, L., Osorio, J.G., Cruise, P., Jones, I., Halbert, G.W., Lamprou, D.A. & Litster, J.D. 2015. Investigation of an 11 mm diameter twin screw granulator: Screw element performance and in-line monitoring via image analysis. *International Journal of Pharmacy* **496**, 24–32.
- Shankali, U.P., Sen, M., Li, J., Litster, J.D. & Wassgren, C.R. 2017. Granule breakage in twin screw granulation: Effect of material properties and screw element geometry. *Powder Technology* **315**, 290–299.
- Sigalingging, R., Herák, D., Kabutey, A., Čestmír, M. & Divišová, M. 2014. Tangent curve function description of mechanical behaviour of bulk oilseeds: A review, *Scientia Agriculturae Bohemicae* **45**(4), 259–264.
- Sigalingging, R., Herák, D., Kabutey, A., Dajbych, O., Hrabě, P. & Mizera, C. 2015. Application of a tangent curve mathematical model for analysis of the mechanical behaviour of sunflower bulk seeds. *International Agrophysics* **29**(4), 517–524.
- Singh, J. & Bargale, P.C. 2000. Development of a small capacity double stage compression screw press for oil expression. *Journal of Food Engineering* **43**, 75–82.
- Statsoft, 2013. Inc, Tulsa, OK74104, USA.
- Uitterhaegen, E. & Evon, P. 2017. Twin-screw extrusion technology for vegetable oil extraction: A review. *Journal of Food Engineering* **212**, 190–200.